MIDI: Obtaining and analysing interferometric data in the mid-infrared

O. Chesneau

Observatoire de la Côte d'Azur, 1 Avenue Copernic, 06130 Grasse, France

Available online 1 July 2007

Abstract

MIDI, and the VLTI in general, is offered as an interferometric system to a wide community of astronomers who do not necessarily have a deep knowledge on how an interferometer works. This text intends to provide the first basics of the MIDI interferometer. It provides a short description of its instrumental layout and a bit of history, followed by an introduction of the data reduction with two software programs: MIA and EWS.
© 2007 Elsevier B.V. All rights reserved.

Contents

E-mail address: oliver.chesneau@obs-azur.fr

1. The MIDI instrument

1.1. Introduction

MIDI was built and commissioned by an association of 12 institutes in Germany, The Netherlands, and France. MIDI is a two-beam combiner instrument dedicated to N-band (8–13 μm) observations. Like any interferometric instrument, it produces raw data in the form of interference fringes.

The mid-infrared wavelength range is also called thermal infrared, because according to Wien's law, a black-body with a temperature of ∼300 K (room temperature) shows a peak emission around 10 μm. The temperatures characteristic for the mid-infrared are thus well below those expected even for cool stars (∼1500 K). Stars emit their light mainly at wavelengths in the visual and the near-infrared. The thermal infrared thus traces photons reprocessed in dusty environments, i.e. the dust absorbs the light from a hot source and reemits it at longer wavelengths. This explains the importance of the N-band (7–13 μm) for the observation and for the improvement of our knowledge of a variety of astronomical objects. In Fig. 1, an atmospheric transmission model for the near- and mid-infrared is shown. The transmission is characterised by a number of molecular absorption bands that define the four mid-IR windows, namely the L-, M-, N- and Q-bands, among which the N band is one of the broadest and cleanest.

The description of this instrument, including its observational procedures has already been described in many conference papers (Leinert et al., 2003a,b,c; Przygodda et al., 2003) and large parts of the PhD thesis of Thorsten Ratzka (2005,[1] in particular Chapters 7, 8 and 9). You can also find a review of the recent scientific outputs in several SPIE conference papers (Ratzka et al., 2006; van Boekel

et al., 2006) or in these proceedings (Tristram, 2007). Of course, we also stress that the reading of the ESO manual for MIDI is highly advised and provides the most up-to-date information of the current status of MIDI.[2] The reader is also invited to visit the MIDI webpage of Christian Hummel.[3] This web page can be used as a first link as it contains all the useful links to MIDI. Moreover, Christian is constantly checking the quality of the data and reports on some technical problems that may occur.

1.2. A bit of history

Six years after the first presentation of the instrumental concept to ESO in 1997, it successfully combined two beams coming from two UTs. A major task of the commissioning and the so-called 'paranalization' of MIDI was to interface it with the VLTI environment. MIDI and AMBER have the advantage of being real VLT instruments, using the same software environment. One year later the observations in the frame of the ESO schedule with objects proposed by the astronomical community started. For ESO period 73 (covering observations from April to September 2004) the process of Call-for-Proposal, of ESO-FORM proposal submission system (phase-1), of Observing Blocks preparation in case of service mode (phase-2) for MIDI was the same as for any VLT instrument. The peculiarity of MIDI comes from the way the instrument time has been offered: as 1-h slots (regardless of the correlated flux of the science target[4]); each slot corresponding to a calibrated visibility spectrum to be measured (fringes on the science target, then on a calibrator). With this scientific instrument at the VLTI a new era in astronomy has begun.
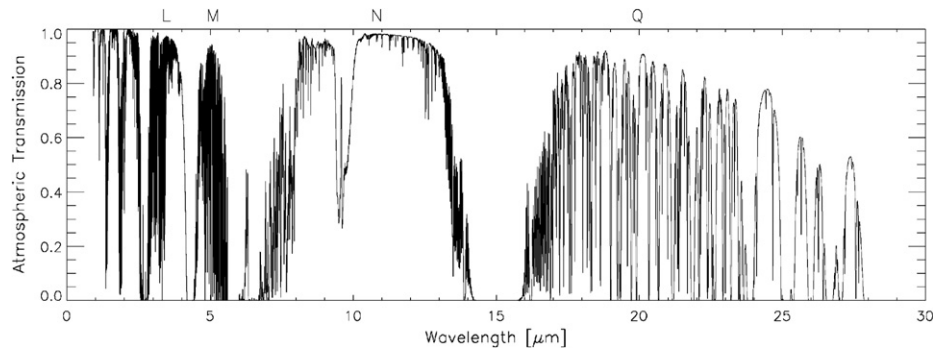

Fig. 1. Atmospheric transmission in the mid-infrared (from Ratzka PhD thesis). Note the broadness and cleanness of the N band compared to other bands. The spectral limits in which MIDI provides good quality data are usually between 7.8 and 13.5 μm. Note also the strong decrease of the atmospheric transmission in the ozone band at 9.7 μm.

1.3. Instrumental layout

The optical concept of the instrument is shown in Fig. 2. From the left, the afocal beams from two telescopes of the VLTI are approaching the instrument through a beam compressor, represented here for simplicity by two lenses. Then, there is a small internal delay line that carries a crucial part of the instrument: piezo-driven roof mirrors that allow MIDI to step the optical path difference between the two input beams rapidly over at least one wavelength within the coherence time of about 0.1 s. Then the beams enter the cryostat (Cold box) through the entrance window (Dewar window). The telescope pupil is imaged by the VLTI delay line optics onto a cold pupil stop to provide the needed suppression of thermal emission from outside the beams. Next, an intermediate focus is formed, where different slits or diaphragms (i.e. spatial filters) can be

introduced for additional suppression of unwanted radiation. Then the beams are recollimated and move on to combine on the surface of a 50–50% beam splitter, situated close to the reimaged pupil plane. The active coating is indicated in Fig. 2 on the lower half of the back side of the ZnSe plate. This is the heart of the instrument. Spectral information can be obtained by spectrally dispersing the image using a prism for low ($\Delta\lambda/\lambda \sim 30$) or a grism for intermediate ($\Delta\lambda/\lambda \sim 200$) spectral resolution (provided that a slit is already inserted in the path). If it is required to monitor the flux in the incoming telescope beams for high precision measurements (the so-called SCI-PHOT mode), beam splitters can be inserted in front of the beam-combiner unit. For this, 30% of the light is extracted and bypasses the beam combining unit. Since the fringe amplitude also naturally depends on the flux ratio of the two input beams, the 'true' visibility can be calculated by taking
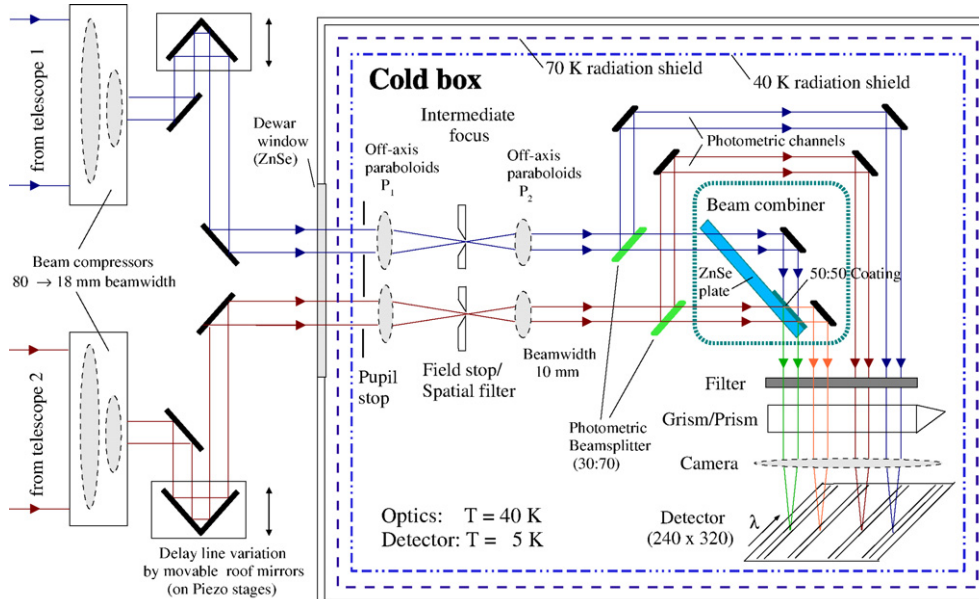

Fig. 2. Schematic optical layout of MIDI (image courtesy of U. Graser, MPIA).

into account the information from the photometric beams since the resulting additional monitoring beams are imaged onto the same detector.

In this type of interferometer, also known as *on-axis pupil plane dinterferometer*, the result of the interference is imaged after the combination in form of two interferometric output channels on the detector (in fact two spectra after the dispersion by the prism or grism). If one of the interferometric channels shows destructive interference of the light, the other shows constructive and vice-versa. This is a natural consequence of the combination of the transmitted and reflected beams, and the conservation of their energy (see Figs. 2 and 4). As we shall see later, the fact that the fringe signal from the source is carried out by two beams in opposite phases is a characteristic that allows us to isolate this signal from the huge background showing the same properties in the two interferometric beams.

1.4. The sequence of observation

The observing sequence for an interferometric measurement with MIDI produces an image of the object at 8.7 μm (default filter), a spectrum from 8 to 13 μm, spectrally resolved visibilities, and correlated fluxes over the same wavelength range. The telescope pointing can normally be done with an accuracy good enough to bring the source into the MIDI field-of-view of $2 \times 2''$. Compared with the signal of, for instance, a $N = 0$ mag object, the flux per arcsec from the sky is about 10 times larger. The photon noise of the background limits the brightness of a source that can be detected. Since the thermal background and thus its noise does not scale with the telescope diameter, it is important to use telescopes as large as possible to increase the signal from the source. The usual way to overcome this problem is by applying a technique called 'chopping'. 'Chopping' means the quick tilting of the secondary (or another convenient) mirror with a frequency of several Hz while images are taken alternately at the two orientations. After the subtraction of the images, the sky background is mostly canceled and mainly the object's signal resides (see Fig. 3). First, for both telescopes used by MIDI the infrared image has to be identified on the detector. These images allow us to adjust the position of the objects to a predetermined pixel in order to maximise the overlap of both images for the following interferometric measurements. This is not always easily done because some of the objects studied are difficult to detect for one of the sensors (guiding or adaptive optics devices), which are only sensitive to optical light. As a consequence, in some (rare) cases, the object does not fall in the MIDI limited Field-Of-View ($2''$) and a 'mosaic' template is needed to find the source around the nominal position.

The integration time of the acquisition frames is only 4 ms to avoid a saturation of the detector by the high thermal background. Therefore, at least 1000 frames are taken with the two telescopes during the acquisition procedure to
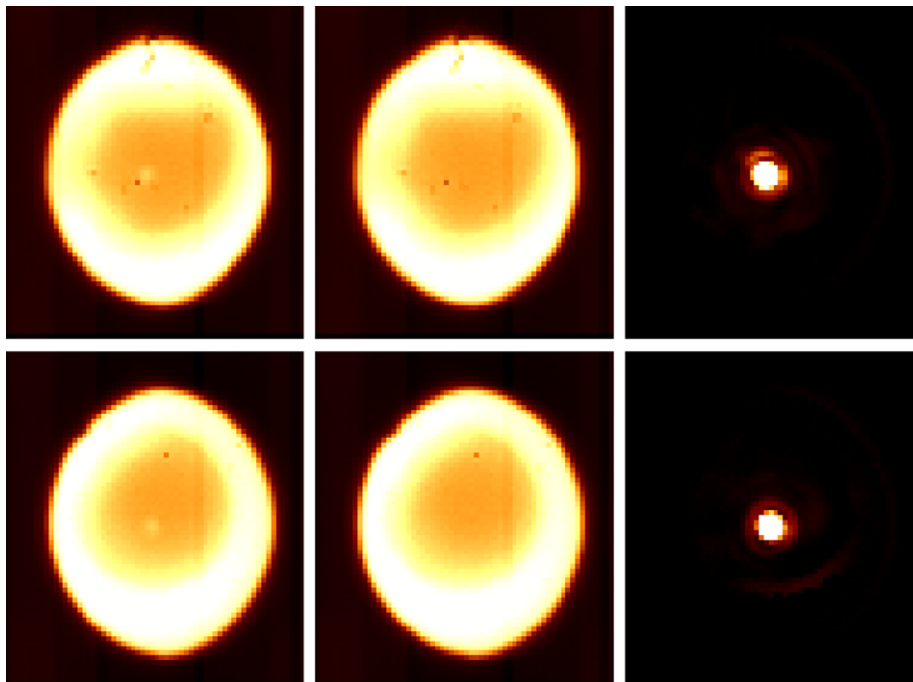
Fig. 3. Example of chopping data for a bright source ($F = 140$ Jy $m_N = -1.4$). The mean of the on-source frames (left), the mean of the off-source frames (centre), and their difference (right) is shown for UT3 (upper row) and UT4 (lower row). Three Airy rings are visible in the upper right image. The bright external regions originate from the tunnels background emission while the darker area delimits the sky background, at colder temperature and less emissive. This dark area is indeed the larger Field-Of-View of the VLTI/MIDI instrument possible from sky acquisition. Note the different shapes and sizes of this FOV for each telescope due to alignment and technical problems (i.e. current absence of variable curvator mirrors). These shapes and sizes depend on the sky position of the source and evolve with time.
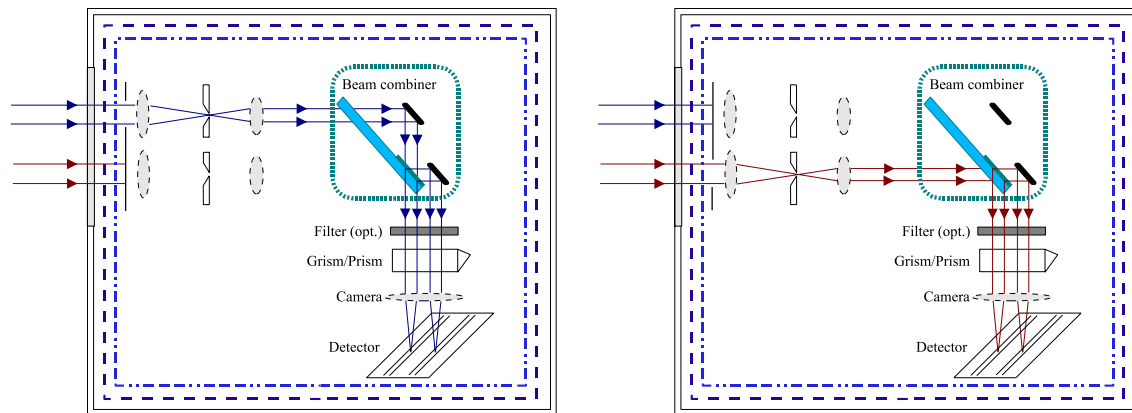
Fig. 4. MIDI optical configuration for the photometric calibration of the visibility that is performed before or after the fringe record in `High-Sens` mode. In order to keep the optical configuration identical to the one for the fringe record, the beam combiner is kept and a shutter allows us to select one of the telescope. The two cases are shown in order to ease the understanding of the way MIDI creates the fringes, and the origin of the 90° flip between the two interferometric outputs (from Ratzka PhD Thesis).

increase the signal-to-noise ratio when combining them.[5] This requires a fast detector readout and a reduction of the amount of data. Only two 62×69 pixels subarrays located where the two beams illuminate the detector are thus read out.

The next step is to search for the fringes, a procedure that is performed after the inclusion of the dispersing device in the beam, either the low resolution prism ($\lambda/\Delta\lambda \approx 30$) or the mid-resolution grism ($\lambda/\Delta\lambda \approx 230$). This spectral resolution allows us to more easily detect the fringes as the coherence length is increased and to obtain *dispersed fringes*, i.e. spectrally resolved interferograms. After finding the location of zero optical path difference (ZOPD) by scanning a few millimeters around the expected point of path length equalisation, an interferometric measurement with self-fringe-tracking is started. In this mode, the piezo-mounted mirrors within MIDI are used to scan a range in OPD of four to eight wavelengths ($\lambda \approx 10\ \mu m$) in steps of typically $2\ \mu m$. At each step, with the corresponding fixed OPD, an exposure is taken which gives the instantaneous value of the interferometric signal from 8 to 13 μm. After each scan of 40–80 μm the position of the fringe packet in the scan is measured and the VLTI delay lines are adjusted in order to recenter the fringe packet for the next scan. For the measurements, the scans can either be kept centered around the white-light fringe (important for MIA data reduction) or at an offset position, which is advantageous for coherent data evaluation (EWS software), where zero OPD crossings present a certain problem. The output after a scan would be the spectrally resolved temporal fringe pattern, which gives the fringe amplitude, or correlated flux. The scans are repeated in saw-tooth manner typically 100–200 times to increase the statistical accuracy. For typical exposure times of 15 ms and readout times of 3 ms this means that the temporal

fringe signal is modulated at a frequency of ≈10 Hz. By definition the visibility is obtained as ratio of correlated flux (from the interferometric measurement) and total flux (from the spectrophotometry). This gives the instrumental visibility, still suffering from atmospheric and instrumental correlation losses. To correct for these losses, the sequence of observations has to be repeated immediately after the object and in the same region of the sky for a source with known diameter, therefore known visibility. The total time for a sequence including object *and* calibrator is 60 min in the ESO rule, but is often much less (∼30–40 min offering some flexibility for the managing of the observations).

1.5. Observing modes

Two main observing modes can be considered, regardless of the spectral resolution used (the low one with the prism or the high one with the grism).

1.5.1. `High-Sens` mode
In the High-Sensitivity mode, the beamsplitters are not inserted in the optical path of the beams before combination, i.e. the photometric channels of MIDI are not used. The photometry is observed AFTER (or in some cases before) the fringe tracking and not simultaneously. Since the fluctuations of the atmosphere affect the photometry of the source at the 10–15% level in a time as short as a few minutes (depending on atmospheric conditions it can fall below 5–8%), the visibility is consequently uncertain by a similar level. *This is by far the main source of error in this mode, and it is not possible to easily decrease it because the knowledge of the level of the fluctuations is lacking.*

For these interferometric measurements no chopping is used, because the two resulting output signals are subtracted from each other as first step of the data reduction, which leads – when supplemented with high-pass filtering – to an efficient background subtraction.

---

[5] For faint target, the number of frames can be up to 12,000–15,000, see Tristam this book for the case of faint AGNs.

In the absence of photometric channels, two exposures are taken with an optical setup (beam combiner, prism and slit) similar to the one used for the fringe exposure: one exposure with the beam A only, then a second exposure with the beam B only (Fig. 4). These photometric exposures allow to derivate the visibility from the correlated flux that has been measured by the fringe exposure. The spectra are recorded on the same pixels of the detector while chopping the secondary mirror of the UTs to remove the thermal background radiation.

1.5.2. `Sci-Phot` mode

Alternatively, two optional beamsplitters (as shown in Fig. 2) reflecting ∼30% of the light into photometric beams can be inserted. These photometric channels can then not only be used to record the spectra, but also to determine simultaneously the position of the beams entering the beamcombiner and to measure the photometric flux to the interferometric signal. In this mode, chopping is necessary while tracking the fringes in order to reliably measure the flux in the photometric channels.

2. Data reduction

2.1. Introduction

For the data reduction, a software package called MIA + EWS can be completely downloaded from the webpages www.strw.leidenuniv.nl/~nevec/MIDI/ or www.mpia.de/MIDISOFT/ or from the webpage of Christian Hummel www.sc.eso.org/~chummel/midi/midi.html.

The software is written in IDL and C but all commands are given in IDL and the user (normally) has no contact to the underlying C routines, which do the hard work. Its first branch called MIA (MIDI Interactive Data Analysis) is based on the power spectrum analysis and works best when the OPD scans are centered on the white-light fringe (zero OPD). The data reduction steps are described in a tutorial on the cited web pages, as well as in Ratzka (2005) and Leinert et al. (2004). Originally, MIA was written to allow the MIDI group at MPIA Heidelberg to have a quick look at the data during the observations on Paranal, or shortly after they arrived in Heidelberg, in order to prepare the next observations.

The second branch of the data reduction system, called Expert Work Station (EWS), uses a clever shift-and-add algorithm in the complex plane, averaging suitably modified individual exposures (dispersed channeled spectra) to obtain the complex visibility $A(\lambda) \cdot e^{i\phi(\lambda)}$. This "coherent" algorithm works best if the OPD scan of the interferometric measurements is offset from zero OPD by about 5λ for low spectral resolution (in order to avoid having only a few dispersed fringes from 8 to 13 μm to characterize the fringe pattern and its delay). It was written by Walter Jaffe at Sterrewacht Leiden and is largely inspired from the MIDI fringe tracker that Walter developed. For a detailed description, see Jaffe (2004) or the documentation on the web page just referenced.

A large part of this tutorial comes from the MIA website and was written by Walter Jaffe, Rainer Köhler and Thorsten Ratzka. The installation is not described in this tutorial and the reader is invited to read the links to the web above mentioned. We insist on the fact that the MIDI web pages are the reference for any command. The MIDI MIA + EWS package is a living software with some commands in the obsolescence process and other in their youth age (i.e. in the debugging stage). However, the core and structure of the code has already been stable for a few years and is rather user friendly. The version described in this text is the version 1.5 of the MIA + EWS package. Note also the useful IDL wrapper of EWS + MIA developed by Christian Hummel that allows you to perform easily tests by switching between both packages rapidly.[6]

2.2. Common features of MIA and EWS: choosing and inspecting the data

In a first step, we want to look what files have been received. Two basic commands are provided. On the one hand a simple IDL procedure that is called make_midi_log. Just type at the IDL prompt

make_midi_log, 'path', LOGBOOK = 'target/filename.log'

where 'path' is the directory where the downloaded files are located. The parameter LOGBOOK specifies the output file. In the default version the procedure reads the keywords providing information about the observed object, the observing mode, the filter, the shutter, the integration time, and the number of exposures (the choice of these parameters can easily be changed by modifying the relatively simple source code). This piece of code is small but useful and you may decide to use it to extract other parameters. I invite you to read and modify it to adapt it to your needs. You can find the source in the /MIA + EWS/MIA directory. It is also a way to learn easily how to extract keywords from the fits files with IDL.

For a fits viewer external to the MIA + EWS and IDL context, I advertise the free software *fv* available at the following link:http://heasarc.gsfc.nasa.gov/docs/software/ftools/fv/.

It works in Windows and Unix environments and is able to handle complex fits formats. This tool should help you to find easily the often complex names of the keyword describing numerous quantities of the observation. These keywords can be called in IDL with the commands you will find in the make_midi_log source.

Another way to get that information 'online' is "Gorgonzola": *files = midigui(dir = 'path')* After a few seconds a window pops up and lists all MIDI-files in the specified directory.

You might have noticed that the number of files is reduced. A MIDI tacking sequence of frames can represent about 500–800 MB of data, and these big files are split into sub-files of about 100 MB each. "Gorgonzola" recognizes files that belong together in one dataset and displays only the first file. If you now select one or more files by marking them in the first column and pressing the "SELECT" button in the upper part of the panel the names of the files are written into the array of files that was specified in the calling command of "Gorgonzola".

A similar routine called with the command *files = midiguis*(*dir = 'path'*) is preferred when handling large numbers of MIDI-files. After the user selected his files the routine writes a binary file to the directory *path*. In this file the displayed information is stored, i.e. next time you start *midiguis* within 'path' the routine quickly reads this file instead of processing all the fits-headers again. Of course, this will not work if you don't have permission to write to the data directory.

If you know which data you want and are too impatient to wait for the GUI to come up, midifile_search can be used. For example, to find all the fringe-track and photometry files of NGC1068 in the current directory, type

files = midifile_search('*.fits',   *OBJECT = 'ngc*1068', *FTRACK, PHOTOMETRY*)

To check what is stored in the variable *files* just type *print, files* or *print, files[i]* to print the files of dataset i.

2.3. Obtaining visibilities in a few commands: `High-Sens` mode

In an ideal world, to obtain reduced visibilities, one would only need to insert to a command the proper files, click in the 'START' button, and then collect the results.

This section describes the basic commands, as close to the ideal world as we can. If the data come from a bright object, with a high level of visibility (i.e. a calibrator), recorded in good atmospheric conditions and without any technical problem, this may work properly. In fact, we are often surprised when it works! The goal of the other sections will be to allow you to get a diagnosis of the data in order to know whether you can trust them, having an idea of the error bars and, in case of bad results, what went wrong. In this case, there are two options: a trickier data handling is often possible thanks to the constant increase of the software capabilities (and the correlated increase of command keywords...) or the data are unrecoverable (which is not a rare case). The detector regions where the fluxes are extracted and weighted are defined from a priori knowledge or from the data in a procedure described in Section 2.6.

2.3.1. MIA software

As a first step start "Gorgonzola" by typing *cal_fileS = midigui*(*dir = 'path'*) where 'path' is the directory where the interferometric and photometric data are stored. Now select the dataset for the fringe tracking (OBS_FRINGE_TRACK_FOURIER) and the two photometric measurements (OBS_PHOTOMETRY_CHOP) by marking the first column and pressing the button "SELECT". Then the names of the files are stored for this example in the array calfile. It is important that the dataset containing the fringes is stored as the first entry in this array. If the photometric observations have been performed before the fringe-tracking was done, please rearrange the array by typing *calfile = SHIFT*(*cal_fileS*,1) Now the main routine of the MIA software package xmdv can be started with *cal = xmdv*(*cal_fileS*)[7] *cal* is an IDL object in which all the useful information for the data reduction have been stored temporarily for this IDL session. Moreover, MIA creates files containing compressed information and some intermediate step information which are used in another IDL session to accelerate the data reduction.

You perform the same procedure with your science target:
sci = xmdv(*sci_fileS*) and you calibrate this visibility:
calvis = sci − > calibratedvisi(*cal,   NAME = name_cal,/ VISPLOT, diameter*).

This calibration is nothing more than the dividing of the raw visibility of the science object by the 'instrumental' visibility or 'transfer function' of the instrument. This transfer function is given by the calibrator visibility corrected for its finite size, that has to be known with a good accuracy if the calibrator is well resolved by the interferometer. If the calibrator is mostly unresolved, the accuracy of this diameter value is less critical.

There is a big chance that you have chosen the calibrator from the ESO website through the `CalVin` database.[8] The diameters of the calibrators in this database are included in the MIA + EWS installation and directly read with the command provided that the 'good' name (an 'HD' name) is put in the NAME keyword. This database can be seen in the file: 'MIA/heidelberg/calibrators.pro'. If the calibrator is not in the list, it is possible to put his diameter in the command.

The calibrated visibility is directly stored in the *cal_vis* vector containing three columns: the wavelength, the bin size and the calibrated visibility.

An important information is still missing for the interpretation of these data: the knowledge of the length and position angle of the projected baseline during the observation. This information is retrieved from the command:

proj_base = sci_file − > baseline()
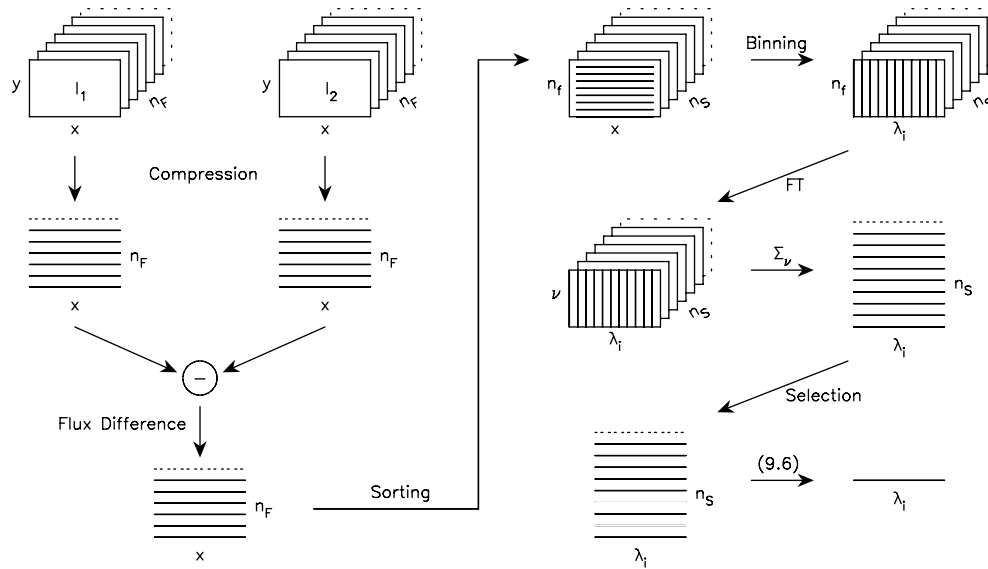;object: HD87643

Fig. 5. MIA software algorithm (from Ratzka PhD Thesis). In a first step two Gaussian masks are created that suppress the areas that lie outside of the central region and are only illuminated by the background. The next steps after multiplying the n_F interferometric frames of I_1 and of I_2 with the masks are schematically presented in this figure. Compression: The frames are compressed in the spatial(y)-direction, i.e. the n_F two-dimensional images in both stacks are transformed into n_F one-dimensional arrays. Flux difference: The one-dimensional arrays originating in beam I_2 are subtracted from those originating in beam I_1. Sorting: The n_F (for instance 8000) one-dimensional arrays are arranged into the $n_S(=200)$ scans in which they have been taken, i.e. $n_f = n_F/n_S(=40)$ arrays belonging to one scan are handled as a unit. Binning: The x-direction, representing the wavelength, is binned by default between 8 μm and the 13 μm into stripes λ_i with a width of 3–4 pixels. Fourier transform: The 1D scans are Fourier transformed and the flux of the fringe peak, corrected from the noise, is extracted. Selection: The value of the Fourier amplitude of the white-light fringe is used as criterion to decide whether a scan can be used for the determination of the correlated flux.

;Baseline: D0–G0
;Date of observation: 2006-02-26T04:33:32.000
;Local Sid Time: 36920.814
;Right Ascension: 151.12620
;Declination: −58.664470
;Projected Baseline
;Length: 31.33 (in meter)
;Position angle: 76.34 (in degree)

The detail of the MIA algorithm is shown in Fig. 5.

2.3.2. EWS software

In EWS, all reduction steps are executed in a Pipeline which gives you a few displays, but saves all the intermediate steps for later diagnoses of reliability.

The only additional required input parameter compared to MIA is a character string, *tag*, which gives a prefix that will be attached to all output files produced by the pipe. This will typically also include a directory. So a typical pipe routine would be called:

tagcal = '/home/reduced_data/calibrator'
midipipe, tagcal, file = *cal_fileS*

If you don't specify the files input parameter, *midiGui* will be called from inside the pipe.

You do the same for the science target: *tagscience* = '/home/reduced_data/science' *midipipe, tagscience, file* = *sci_fileS*

Then you calibrate with: *midiCalibrate*, *tagscience*, *tagcal*

This last command creates an impressive amount of output files; all of them in the FITS format (except one in PS format that contains all the useful graphs allowing you to check the data quality). The information of the projected baseline is also included. Note that the OI-FITS format files can be read by EWS IDL routines but can also be exchanged and proposed as public data since the OI-FITS format is becoming the official one for the optical interferometry techniques and is described in Pauls et al. (2005). Information can be found in the OLBIN website[9] or directly the OI-FITS site.[10]

2.4. Obtaining visibilities in a few commands: Sci-Phot mode

As said previously, the Sci-Phot mode provides a simultaneous photometry to the interferometric data. But this mode also involves another crucial difference: in order to remove the background from the photometric beams, it is necessary to perform the fringe observations with chopping. This has certainly represented one of the most difficult challenge for the MIDI consortium: the MIDI observations have to be synchronized with the incompressible clock that is the observing time of one single frame, i.e.

---

[9] http://olbin.jpl.nasa.gov/software/index.html.
[10] http://www.mrao.cam.ac.uk/jsy1001/exchange/.

the exposure time plus the read-out time (~15 mas with prism). Then the piezo moves step-by-step between two frame exposures, coming back to its zero position after each scan of about 40–80 frames, and, *synchronously*, the chopping mirror (i.e. the UT secondary mirror, 50 kg, 1.1 m) points toward the source of the sky with an approximate rate of 0.5–1.5 Hz (corresponding to one scan on source for one scan on sky).

2.4.1. Cross-coupling coefficients

It is necessary to calculate the cross-coupling (also called κ) coefficients between the interferometric I_1, I_2 channels and the photometric P_A, P_B channels. We don't know yet whether these are stable for hours, days, years but the first studies suggest that they should be at least stable on a day to weeks scale.[11] To calculate the coefficients you need standard chopped photometry data (i.e. with AOPEN and BOPEN shutter settings, taken with the NRTS mode DEFAULT_CHOP[12]) on a BRIGHT calibrator. Another promising method is to use the sky background itself to compute this quantity (keyword */sky*) since in N band the sky flux is very large. This way of computing the coefficient is currently being tested and the reader is invited to look regularly at the web site to be aware of the latest developments of the software. The command is the following

midiCrossCoeff, base, files,/sky

base is a character string containing the beginning of the output file name, including directories, e.g. *base = '/home/user/testdata/cc'*, in which case the output file is */home/user/testdata/cc.crossCoeff.fits*. files is an array of two character strings, describing the AOPEN and BOPEN data as delivered by *midiGui*.

The output file is a standard IMAGING_DATA table (the natural format of MIDI files) with 4 rows containing a single DATA1 array, representing the ratios I1/PA I1/PB I2/PA and I2/PB. You can read it in with *oirGetData*.

2.4.2. MIA software

To reduce this kind of data with MIA type: $x = obj\_new(''xmidispvisi'', file, cross = crossFile)$

Note that you cannot use *xmdv* because it will search for photometric files and use them, *even if you don't specify any*.

MIA is using the same programs as EWS to convert the PA + PB data to I1 + I2 data, and runs the standard masked photometry reduction on this data. What the program does is to resample the PA + PB data onto a grid so that it looks like the I1 + I2 data, and then runs the standard masked photometry reduction on this data (see Fig. 5). Under these conditions, the discrepancy between the two softwares do not originate from the photometry of the source, but from the computation of the correlated flux (for which the algorithms are totally different). Note that the photometry obtained in High-Sens mode for the two softwares is also identical now (i.e. with the version 1.5 of the package, this was not true for earlier versions).

2.4.3. EWS software

To reduce data in this format with EWS type: *midiSPipe, base, file, cross = crossFile*

where base is the usual string, file is a single string, describing the ABOPEN data taken in interferometric mode (i.e. your DISPERSED_FRINGE_TRACK data recorded with both telescopes light). The output is the usual array of files base.corr.fits, base.photometry.fits... plus some new intermediate result files like *base.Aphotometry.fits*, *base.ABphotometry.fits* (see Fig. 6).

2.5. Working with the MIA GUI

As said above, MIA was first intended to *inspect* the data and we invite you to use it to get familiar with the kind of data that MIDI provides. The following introduction is extracted from the web, and regularly updated. The last update can be found at the following link:

http://www.strw.leidenuniv.nl/~koehler/
MIA+EWS-Manual/mia_gui.html
The most complete way to visualize the results is to bring up the main graphical user interface (gui). The gui is called by the following command: $cal \rightarrow gui$ or $sci \rightarrow gui$
A big window should appear. On some computers the color management of IDL is very sophisticated. If you do not see colours please try: $cal \rightarrow gui,/tru$

This will use 24 bit colors and might help. In some cases it was useful to close the gui and restart it again. All the modifications are recorded and thus available afterwards.

The graphical user interface is divided into various areas and subpanels. Some of them are interactive.

2.5.1. OPD panel

This is the top panel, occupying the full window. This panel displays the optical path difference (OPD) vs. the frame number. Clearly visible is the jump of OPD (in red) that allows us to measure the noise far outside the Zero OPD position where the fringes are supposed to be, and the tracked part (in green) that shows the OPD position during the tracking of the fringes. This OPD step

---

[11] The stability of the MIDI instrument is related to the stable physical conditions in its cryostat. If the stability would be shorter than hours, there would be no point in doing SCI_PHOT mode).

[12] This means selecting the telescope beam entering the A or B MIDI entrance, and ensuring that these data were recorded while the chopping mode was on.
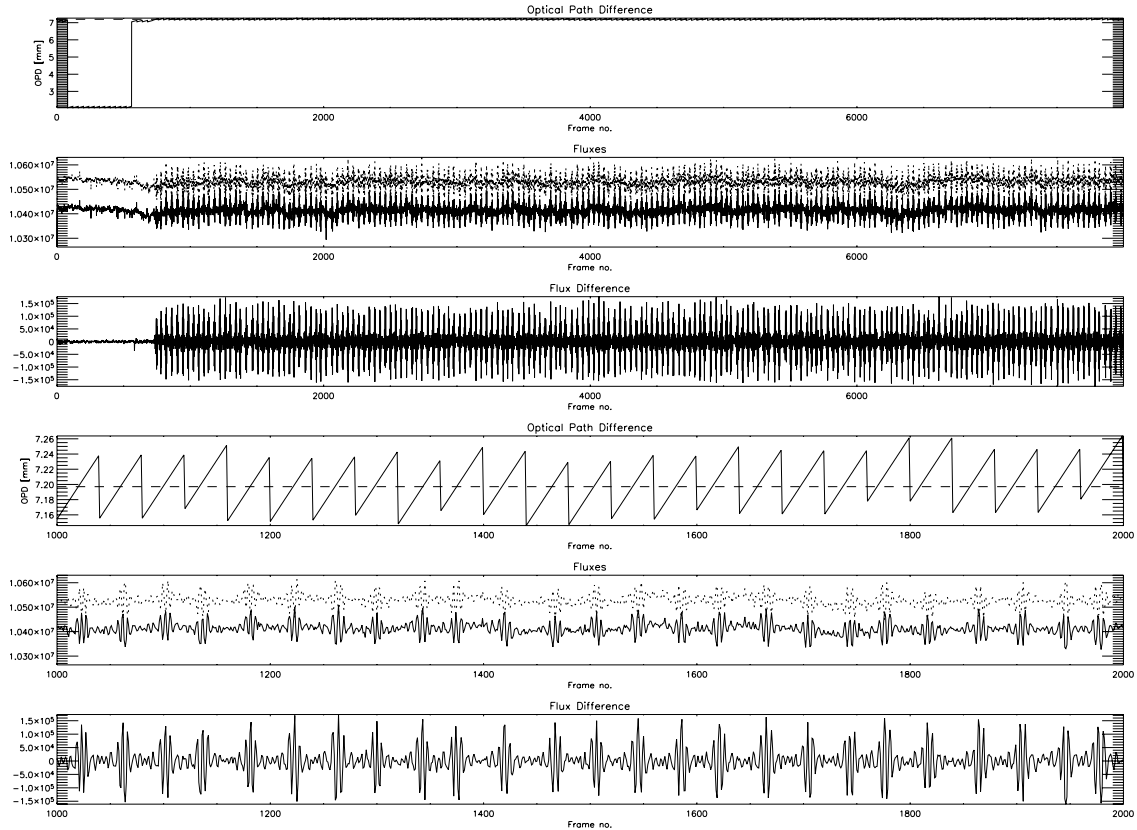
Fig. 6. Part of the MIA GUI representing from top to bottom: the OPD Panel in mm (top, abcisse axis in frame number n_F), the level of the flux extracted for each telescope in counts, the difference of these flux illustrating the efficient removal of the background and the fringe signal in anti-phase emerging strongly, a zoomed view of the OPD Panel showing the scans of the piezo super-imposed to the OPD residuals of the tracking, the fluxes from each telescopes with the fringes in anti-phase and their difference. Figure from MIA web site and Ratzka PhD thesis.

destroys the scale of OPD that would be useful to check the quality of the track. You can change this scale by clicking on the panel. A small window will pop-up allowing you to change the parameters of the plot. With a right scaling, the 60–80 μm scans of the MIDI piezo are clearly visible. During each of the 200–400 scans, 40–60 exposures have been taken leading to a total amount of 8000–12,000 frames (or even more) (see Fig. 7).

The quality of the tracking is indicated by the smoothness of the OPD curve. Usually, jumps in the curve coincide with a loss of fringes, which can immediately be seen in the panels below.

2.5.2. Photometry panel
This panel displays the measured flux vs. the frame number. To get the photometry vs. the pixel number type:

spec = *cal* → *photometry*()
print, *spec*

One gets a 3 by *N* array, where *N* is the number of bins in lambda defined by default or by the user (see following section). The Keywords /Atotal and /Btotal return the sum of the two (I1 and I2) A- or B-spectra, respectively. Everything is in ADU/sec (conversion factor for MIDI:∼ photons/ADU). The command

lambda = *cal* → *lambda*()

returns an array that gives wavelength in *m* as function of the pixel number. With

cal − > *set_lambda*, *lambda*

the user can set his own wavelength calibration if needed.

2.5.3. Fringe panel
This panel displays the flux difference (I1 and I2) vs. the frame number, i.e. the modulation in the correlated flux. Before MIDI reached zero OPD no fringes are visible. Afterwards, a strong signal could be detected. By typing

cf = *cal* → *correlflux*()

One gets the correlated flux as function of wavelength. This is a 3 by *N* array, where *N* is the number of bins in lambda. The first row (*cf*[0, *]) is the wavelength in the center of the bins, the second row (*cf*[1, *]) is the width of the wavelength bins, and the third row (*cf*[2, *]) is the correlated flux in ADU/sec.

Keyword /*PLOT* will plot the good and bad fringes in the lambda bins, and the correlated flux. Keyword /*CFPLOT* will plot only the correlated flux.
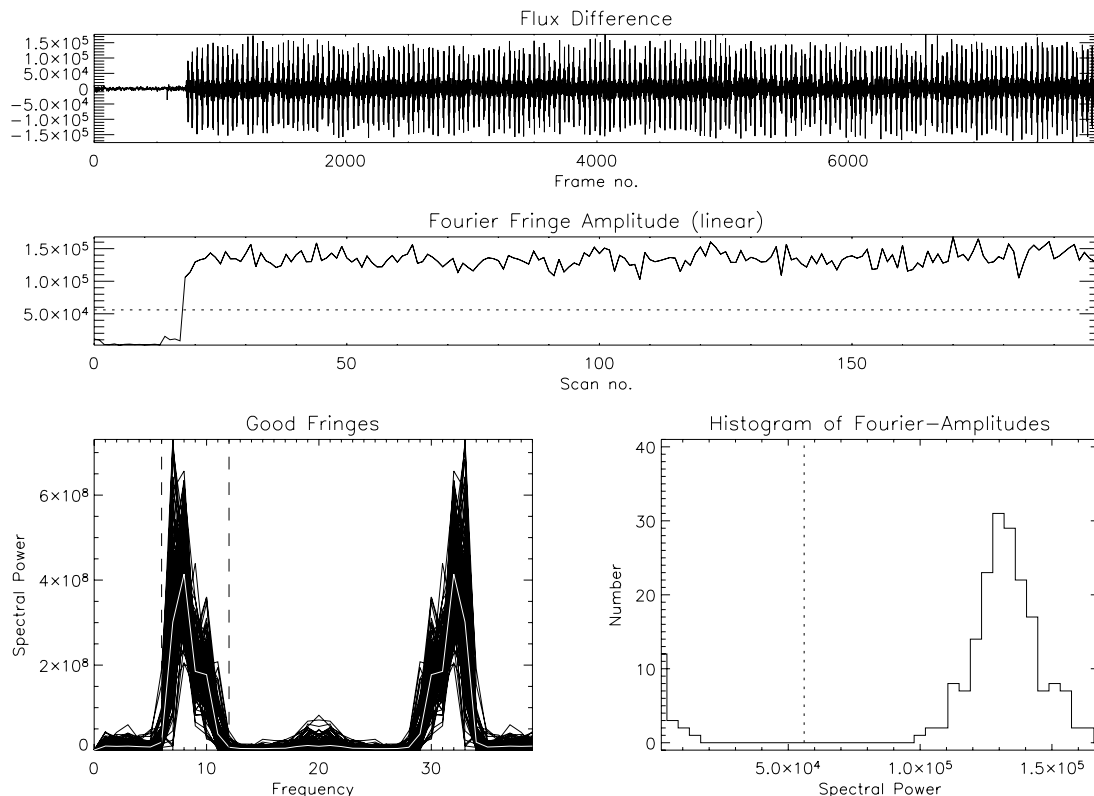
Fig. 7. Part of the MIA GUI representing the flux difference between the I1 and I2 beams in counts (top, abcisse axis in frame number n_F), the level of the correlated flux estimated for the full N band from the Fourier transform of each scan (middle, abcisse axis in scan number n_S), the Fourier peaks Panel (bottom left) and the Histogram of the Fourier-Amplitudes (bottom right). Figure extracted from the MIA web site.

To set the binning in wavelength one can use the command

$$cal \rightarrow set\_lambda\_bins, \, start, \, end, \, step, \, width$$

where *start* is the number of the first column used, *end* the number of the last column used, *step* the spacing between bins, and *width* the number of columns added for one bin. For example

$$cal \rightarrow set\_lambda\_bins, \, 0, \, 100, \, 25, \, 50$$

will set the bins 0…49, 25…74, 50…99, 75…124, and 100…149 pixels. Please notice that a bin can extend beyond the given end column. An interactive tool to define the bins is the "LAMBDA GUI". It can be started from the menu or with

$$cal \rightarrow lambda\_gui$$

2.5.4. Fourier fringe amplitude panel

This panel displays the maximum Fourier amplitude (FA) of the fringes in the white light, i.e. integrated over wavelength vs. the scan number. To get the amplitude, we integrate over wavelength, Fourier-transform each scan, add up the power spectrum at the frequencies where we expect fringes, and calculate the square root (see the section below on the display of the scans Fourier transforms).

2.5.5. Fourier peaks panel

The spectral power of the good and the bad fringes vs. the frequency is plotted on the lower left panel of the GUI. The vertical dashed lines mark the frequency range where fringes are expected, i.e.

$$v_{min} = \text{floor}(\delta/\lambda_{max} + 0.5)$$
$$v_{max} = \text{floor}(\delta/\lambda_{min} + 0.5)$$

where δ is the length of a scan. The symmetry of the plots, i.e. the right side is a mirrored left side, is a consequence of the fast Fourier transform algorithm. By clicking onto the plots, a window opens that displays the plots for the different wavelength bins set by default or by the user with the "LAMBDA GUI" or the corresponding command set_lambda_bins. The good fringes are plotted on the left side, the bad fringes on the right side. The frequency range, where the fringes are expected moves from lower to higher frequencies, because the binned wavelengths are decreasing. Another window opens simultaneously that shows the 'instrumental' visibility of the object, i.e. the visibility observed uncorrected from the instrument transfer function.

In order to determine the instrumental visibility, i.e. the visibility of an unresolved point source, we use a calibrator object of known diameter with the routine

$$insvis = x \rightarrow instruvisi(diameter, NAME = name)$$

where diameter is the diameter of the calibrator in mas. If the object is listed in the calibrator database, the diameter can be omitted. The name that is used to find the object in the database is either read from the MIDI data files (can be checked with $object = cal \rightarrow get\_objectname()$) or can be given with the parameter NAME. The instrumental visibility is calculated by dividing the raw visibility with the expected visibility of the calibrator. When /VISPLOT is specified one gets a plot of the instrumental visibility, i.e. insvis[2, *] vs. insvis[0, *]. The parameter /PLOT launches the display for the wavelength-binned spectral power of the fringes.

2.5.6. Info panel

This panel contains all the useful information of the signal. All the numbers are derived from the integration of the spectrally dispersed signal over the full band defined with the "LAMBDA GUI". Note that this integration currently does not take into account the distortion of the beams. This distortion is rather small with the prism but is large with the grism. As a consequence, the numbers displayed in this panel are only indicative of the signal but cannot be used for a scientific application. Only the dispersed visibilities are the true scientific signal.

2.5.7. Histograms of Fourier-amplitudes and mean optical path length

On the lower right panel two histograms are drawn. One displays the distribution of the scans with respect to the Fourier amplitude and the other with respect to the mean optical path difference. Three thresholds can be set.

(1) Threshold for "good" scans, i.e. scans that contain fringe signal (solid vertical line in FA-histogram, dotted upper horizontal line in OPD panel).
(2) Threshold for "bad" scans, i.e. scans that do not contain any fringe signal and can be used to estimate the noise (dotted line in FA-histogram, dotted lower horizontal line in OPD panel). However, the amplitude used with this threshold is measured in "white light", i.e. with a bandwidth of about 5 μm. In dispersed mode, the bandwidth of the individual bins is smaller, therefore the fringe packet is wider (in OPD-space). This means that one can detect fringes at larger distances from the zero OPD, and therefore the "white light" threshold will not exclude all scans with fringe signal. So, do not set this threshold to anything but 0, use the next threshold.
(3) Minimum distance of "noise scans" from the median OPD in meters (solid vertical lines in the OPD-histogram). Scans with a mean OPD that is more than this distance away from the median OPD of all scans are used to estimate the noise in the power spectrum.

These thresholds can be set either interactively by dragging the lines in the histograms with the mouse pointer, or on the IDL prompt by the command

$$cal \rightarrow set\_thresholds, good, bad, noiseopd$$

where noiseopd is optional. To read out the current values type

$$th = cal \rightarrow get\_thresholds()$$

The percentage of good and bad scans with the current thresholds is returned by

$$gb = cal \rightarrow get\_percent\_goodbad()$$

2.6. A critical step of both softwares: using and making MASKS!

MIDI does not currently use spatial filters and the light of the target has to be isolated and extracted from the detector. Even though chopping is used, the target is often immersed in background residuals and in order to minimize that noise, it is important to put a greater weight in pixels for which the target is brighter. Both MIA and EWS use *masks* for this. A *mask* is a file containing information that defines the target position on the detector and the weight to apply for the extraction and collapse of the data from a 2D flux distribution to a 1-D spectrum. A 'mask' is composed of 2 windows in `High-Sens` mode, 4 in `Sci-Phot`, about 40 pixels in the spatial direction (that includes parts of the detector receiving no light from the sky), and 100/300 pixels in the spectral direction for low/high dispersions, respectively. Masks contain images with values between 0 and 1 that tell which pixels of the MIDI data should be used (and what weight should be attributed to them – the values in the mask are floating-point numbers). They are stored in files with the same format as MIDI data.

One could think that managing mask is an easy task but in the short MIDI history it has been the main source of (human or software induced) errors (besides the photometric instability inherent to the mid-IR domain).

Two different approaches were tested: fixed masks and masks fully defined from a set of data. Both approaches have their drawbacks. A fixed mask is not versatile enough to adapt to several changes of the beams properties: their position in the most usual cases and often also their FWHM. Before the outcome of the adaptive optics device MACAO, the FWHM of the beams was very seeing dependent. Since then, it is more stable but the position of the beams is still subject to fluctuations. The beam images are often spread in the vertical direction by more than 3–5 pixels (i.e. 300–400 mas), corresponding to more than the expected FWHM of the diffraction limited Airy spot, even though the adaptive optics loop is closed. In general,

this is due to the remaining motion of the beam into the tunnel, chopping or active optics technical problems.[13] Moreover, the fine positioning step of the pointing is sometimes not satisfactory and the beams of the telescopes are not well centered (and often in this case, not overlapped properly). A mask could be generated from the data. Until recently, this was the approach preferred for the MIA software. The trace and the FWHM of the beams were computed based on 1D Gaussian fitting for each spectral channel of the photometric beams, and also the image of the rms of the interferometric channels (containing the location of the fringes, i.e. the correlated flux and not the total flux that might be at a different location for different telescopes). This approach often appeared rather satisfactory, but in many cases for which the SNR of the data is too low, the quality of the mask parameters was decreasing drastically, leading to strongly biased visibilities.

An intermediate approach is under study involving a fixed mask with a well-controlled shape and FWHM. The only free parameter fitted on the data are its vertical position allowing us to take into account an offset of the beams during the acquisition. There is currently a C-program (*oirShiftMask*) and an idl script (*midiShiftMask*) that compute a new mask from an old one by estimating the optimum shift in the spatial-direction. In EWS, these can be called automatically for `High-Sens` data with the */shift* parameter in *midiPipe* but this command can also be used to change the maskfile in the MIA software (*MASKFILE = filename* keyword). There should be soon a convergence for the methods creatings masks used both by MIA and EWS.

2.7. Extracting images and spectra

The first recorded data are the acquisition frames used to determine the correct positioning of the images of the target on the chip. These diffraction limited images can be of excellent quality since the MACAO adaptive system provides an excellent correction in the N band, and they can be used scientifically for two purposes: a flux calibration in the filter used and to check whether the science target is resolved by the beam of a 8 m telescope. In the N band regime, this case is encountered more often than usually guessed by observers. This is particularly true for Young Stellar Objects and Evolved stars. The way of reducing these images is classical: extracting the chopping images from the source and several calibrators, flux calibrating and studying the parameters of the calibrator beams (point spread functions, PSFs) versus the source one (FWHM, ratio minor/major axis, temporal stability...). The reduction of these images is not the direct goal of the MIA + EWS package, but useful utilities allow us to do it (see the web pages for further information).

The flux calibration of the spectra is almost always necessary for the scientific interpretation of the MIDI observations. The MIDI calibrator can almost always be used for this (but the latest types M3–M5 are not advised). Both MIA and EWS can provide the photometry of each beam in ADUs (see Section 2.5.2 for MIA). We stress that the target and calibrator spectra have to be recorded at close airmass (i.e. typically ±0.2) and this is generally the case. An airmass correction is difficult to perform with the existing MIDI mode of operation. It would imply recording spectra of the same source at different airmass and would hamper the time efficiency of MIDI for recording fringes, its primary goal.

A list of primary calibrators is available in the ISO database.[14] A part of these calibrators are also MIDI calibrators for interferometric observations. It has been proved very useful to observe these calibrators for calibrating simultaneously spectra and visibilities and an extracted list is available in the MIDI webpages.[15] Note however that the Cohen calibrators are rather faint (5–15 Jy) and cannot be used for ATs observations.

If the target is a primary calibrator, then the calibration is straightforward: $\mathrm{Targ}_{Jy} = \mathrm{Cal\_template}_{Jy} * \mathrm{Targ}_{ADU} / \mathrm{Cal}_{ADU}$.

If the target is NOT a primary calibrator, the best is to use as reference the IRAS flux of the object and use a Cohen template of similar spectral type for the continuum correction:

$$\mathrm{Targ}_{Jy} = \mathrm{Template}_{Jy} * \mathrm{F12}\mu m_{Cal} * \mathrm{Targ}_{ADU} / (\mathrm{Cal}_{ADU} * \mathrm{F12}\mu m_{template}).$$

The IRAS flux of the Cohen calibrator is written in the header of the template file.

3. Detecting and interpreting problems

This section shall probably be far from exhaustive. We try to make a small list of criteria to assess the quality of the data. Reducing MIDI data is not trivial (even for enlightened pan-dimensional beings) and there are many things that can go wrong in the programs.

We stress that most of the tests can be performed by checking the data with the MIA GUI for instance. We also insist that the best way to find a misbehavior of the VLTI + MIDI instrument is to cross-calibrate several calibrators.

Of prime importance too, in case of doubts on the results, is too perform a data reduction with both MIA and EWS. This is a great chance of the MIDI user to have two independent way of reducing the data. If the results of

---

[13] The adaptive optics are situated *below* the UTs, much earlier than the MIDI instrument.

[14] http://www.iso.esac.esa.int/users/expl_lib/ISO/wwwcal/isoprep/cohen/templates.

[15] http://www.eso.org/instruments/midi/tools/spectrophot_std.html.

MIA and EWS are different, it means that at least one of the results is wrong, so you should be happy you noticed that before you published it. You have to inspect the data and note unusual intermediate results in both softwares.

A problem often encountered is the use of a bad mask. If the results depend on the mask, but not on the program used, then one of the masks is not appropriate for the data. Your mission, should you choose to accept it, is to find out which mask is better for *your* data. This has been the subject of discussions among the MIDI experts, as witnessed by the totally different strategies used by former versions of MIA and EWS, but a satisfactory solution has emerged (see devoted section). The common origin of such a problem is a bad alignment of the telescope beams and this implies often that the overlap of the beams from both telescopes is not satisfactory. As a consequence, most of the time these kind of data, potentially biased, have to be discarded from the scientific interpretation.

The estimation of the total flux should not be different, since MIA and EWS use now the same program to measure it. It is possible, however, to override this in MIA with the NOEWSPHOT-switch, which may or may not be a good idea. The alternative code does not do a very good background subtraction, so its results for faint sources are almost certainly wrong. However, this should not matter for bright sources, and sometimes funny things happen to the background, which can cause EWS to go crazy.

Another large field of potential reduction problems is when one deals with faint targets. This particular case is treated below.

3.1. ReduceNight

This routine is designed to assist the user when reducing whole nights of observations. This routine is important to detect sets of data with potential problems and will be even more interesting in the frame of large observing runs performed with the ATs. The strong point is that it allows us to manage the data reduction of science objects reduced with different calibrators.

The routine does not turn everything into a "black box", but just simplifies the bookkeeping and the repeatability by calling "MIA" with the correct filenames and by storing the results.

> *reducenight*,'⟨*path*⟩'
> Options:
> /*CALONLY* required for nights with calibrators only
> /*STEP* set the spacing between the visibility bins to 1, i.e. maximum sampling.

'path' is the directory containing the data to be reduced. The procedure creates logfiles of this directory with *make_midi_log* and identifies all tracking and photometric files by using the NRTS_MODE keyword. After the identification, a window is displayed (see corresponding web page). It contains a diagram where all found tracking (top) and

photometric files (bottom) are plotted versus a time axis. Files identified by the observation time as part of one dataset are connected by a line. The name of the observed object is printed in red.

Afterwards, this program allows us to edit a Tracklist of all the observations performed in the night, can reduce them and calibrate them by using different calibrators chosen by the user.

The reader is invited to go to the following web page for detailed information: www.strw.leidenuniv.nl/~koehler/MIA+EWS-Manual/mia_rednight.html.

3.2. Visibilities larger than unity

In order to detect this kind of problem in the raw visibilities, you should get familiar with the typical MIDI transfer function. The MIDI transfer function should be close to a straight line from visibilities of the order of 0.5–0.7 at 8 μm to 0.6–0.85 at 13 μm. This curve is strongly dependent on the way the extraction of the total and correlated fluxes is performed, and is somehow a signature of the extracting software.[16] Transfer functions above these values indicate that the estimation of the total photometry is somehow under-evaluated. As soon as the calibrator magnitude is comparable to the science one, both targets should be affected by the same bias of extraction and the visibilities estimated by the division of the science instrumental visibilities by the transfer function from the calibrator should be more of less independent from this problem. This is the kind of tests usually reported in the MIDI publications when MIA and EWS independent data reduction are compared and agree.

Nevertheless, it is always useful to have a look into the raw visibilities and to check whether they are close to or above unity. This is always the sign of a bad observation or a problem in the extraction of the photometry. It must also be noted that for MIDI the estimation of the total photometry is more often the cause of the problem rather than the estimation of the correlated flux (except in the case of very low visibilities). This is due to the fact that chopping is necessary for estimating the first one, and that the background fluctuations encountered in the N band can degrade the estimation of this quantity. Thanks to the modulation of the fast piezo scanning, the estimation of the correlated flux is more robust. Raw visibilities greater than unity means that the photons from the source are not well extracted from the background. Usually, the source is faint, but it could also be related to a chopping problem during the photometry record. Check the 'ESO HIERARCH ISS CHOP THROW' keyword, which, when set to zero, indicates a problem with chopping. The chopping throw parameter defines the distance between the source and

---

[16] Of course, an ideal data reduction software should be 'transparent' but we live in a real word in which the choice of an algorithm has an impact on the data reduced.

sky pointing direction. This reduces the flux in the chopped spectrum and consequently leads to a normalization of the fringe spectrum with a flux too small, causing larger than real visibilities (the reader is invited to regularly visit the webpage of Christian Hummel that reports on this kind of problems).

3.3. Dealing with weak sources

We have seen that problems often arise when the total flux estimation is wrong. We note that the behavior of the MIA and EWS softwares are different only for the estimation of the correlated flux: in the case of MIA the estimation of the correlated flux is independent for each spectral channel whereas EWS deal with the full dispersed channeled spectra, and benefit from this information, decreasing the level for which well calibrated correlated fluxes can be extracted. Good example of MIDI data on faint sources can be found in the contribution from Tristram (2007, this book).

3.3.1. Overestimated visibilities at the edges of the N band

This is probably related to the underestimation of the total flux of the faint science target when the SNR is too low whereas the brighter calibrator visibility is correct. An easy way to check this is to change the binning of the data reduction process. This is especially true in the case of the grism data: if the source is weak and the binning too small, the estimated flux can be noisy but also strongly biased. The default binning parameters of MIA are 3, 1 implying that spectral channels of 3 pixels by step of 1 pixel are used. It is possible to set the binning parameters to larger values. If the visibility curve is stable whatever the binning parameters used (not too large of course), this is an indication that the photometry is reliable. If not, the best curves should be the ones with the largest bins, i.e. the lower set of visibilities.

3.3.2. The ozone absorption feature

The ozone absorbing feature is centered at 9.7 μm (see Fig. 1). The decrease of the flux is such that sometime no information can be extracted in this band, or strong bias of the softwares appear. The best way is to remove these points. We stress that any signal with a strong departure from the continuum signal could possibly originate from the silicate feature commonly encountered in the chosen science target. The spectral region affected by the ozone feature should perfectly follow the width of the ozone feature that is narrower that the signal from the broader silicate feature. This is the best way to decipher the origin of such a signal.

3.4. The difficult estimation of error bars

The reader is invited to read Section 4.4 'Errors and biases' written by Guy Perrin. Here, we present briefly the main sources of error in the mid-IR.

3.4.1. High-Sens mode

As said previously, in this mode the photometry is performed about 3–6 min after the record of the fringes, i.e. the correlated flux. Therefore, the photometry recorded does not correspond to the flux from the source at the time of the record of the fringes, and this leads, in a highly fluctuating mid-IR, to an uncertainty of the order of 7–15% in the usual cases. This error depends critically on the atmospheric conditions in the night or part of the night including the observation of your science target. It is easy to get an idea of the quality of the night by searching the atmospheric parameters (seeing, wind speed, coherence time τ_0...) in the header of the fits files or in the ESO ambient conditions data base[17] that allows you to get a clear view of the full night. A good estimation of the error bars is obtained by comparing the transfer function (i.e. the instrumental visibilities) of 3–6 calibrators observed closely to the source and computing their rms. The command *ReduceNight* is made for this.

The errors estimated from the calibrators transfer functions are multiplicative. A 15% calibration error level for a science target with an observed visibility 9iV of 0.95 leads to the following estimation: $V = 0.95^{0.14}_{0.12}$. If the visibility of the science target is $V = 0.01$ then the contribution of the multiplicative calibration errors leads to: $V = 0.05^{0.0075}_{0.0065}$. This is unrealistically low. In fact, when we estimate the MIDI error of your measurements in the previous case, the main source of error is identified but there are many different sources. In the case of low visibility measurement, the main source of error is the error on the estimation of the correlated flux that can be high, especially in the case of the MIA software since the flux extracted from the peaks of the Fourier transform of the scan has to be corrected for the additive noise inherent to this method.

A way to estimate this additive error is to use the histogram of the correlated flux in the scans (Section 2.5.7) to estimate the rms of the value extracted for science object, compared to the rms of the calibrator one.

3.5. Sci-phot mode

A much better accuracy of the measurements is expected with the simultaneous record of the photometry during the scanning of the fringes. Nevertheless, compared to the previous situation, new sources of error are added: the photometric beams fall in different parts of the detector than the interferometric ones, they are more distorted and the flux is lower compared to the `High-Sens mode`.

The quality of the calibration relies on a new quantity: the estimation of the flux ratio between photometric and interferometric beams carried out by the cross-coupling coefficients. Currently, the cross-coupling coefficients are supposed to be very stable since their potential variations are essentially determined by the very stable physical conditions in the MIDI dewar. Currently, the knowledge on

---

[17] http://archive.eso.org/asm/ambient-server.

their value is mostly limited by the quality of the measurement at the 1–3% level.

In this mode, the budget of errors is probably more balanced between several different sources. As usual, as the accuracy of an instrument increases, a broader range of errors has to be considered: the error of the estimated calibrator diameter.[18] the statistical error on the correlated and total flux of the source and the calibrator ...

The algorithms for the MIA and EWS reduction of this kind of data have not been fully tested yet. We invite any user of the softwares to critically test the quality of the reduction in the usual way, by cross-calibrating the observation of different calibrators. Any strange behavior have to be reported to the MIDI consortium via Walter Jaffe,[19] Rainer Köhler[20] or Olivier Chesneau.[21]

Acknowledgements

References

Jaffe, W.J., 2004. SPIE 5491, 715.
Leinert, Ch., van Boekel, R., Waters, L.B.F.M., et al., 2004. A&A 423, 537.
Leinert, Ch., Graser, U., Richichi, A., et al., 2003a. The Messenger 112, 13.
Leinert, Ch., Graser, U., Przygodda, F., et al., 2003b. Ap&SS 286, 73.
Leinert, Ch., Graser, U., Waters, L.B.F.M., et al., 2003c. SPIE 4838, 893.
Ratzka, T., 2005, PhD Thesis, University of Heidelberg.
Ratzka, T., Chesneau, O., Meisenheimer, K., Tristram, K., 2006. SPIE 6268, 20.
Pauls, T.A., Young, J.S., Cotton, W.D., Monnier, J.D., 2005. PASP 117, 1255.
Przygodda, F., Chesneau, O., Graser, U., et al., 2003. Ap&SS 286, 85.
van Boekel, R., Abrahám, Péter, Correia, S., et al., 2006. SPIE 6268, 13.

---

[18] This is particularly true in the case of observations with ATs. Bright and therefore extended calibrators have to be observed, and the error on their diameter can be large.

[19] `jaffe@strw.leidenuniv.nl`.

[20] `R.Koehler@lsw.uni-heidelberg.de`.

[21] `Olivier.Chesneau@obs-azur.fr`.